Diffuse scattering from quasicrystals

Marko V. Jarić
Center for Theoretical Physics, Texas A&M University, College Station, Texas 77843-4242

David R. Nelson
Department of Physics, Harvard University, Cambridge, Massachusetts 02138
(Received 22 July 1987)

A theory of both thermal and quenched diffuse scattering from incommensurate crystals and quasicrystals is developed. We explore, in particular, the effects of strain fluctuations due to phasons which have dropped out of equilibrium at high temperatures, providing a source of quenched, spatially varying disorder. The theory leads to anisotropic peak shapes, in analogy with Huang scattering in ordinary crystals. In contrast to Huang scattering, the peak shapes vary greatly along a given direction in reciprocal space. Analysis of peak shapes can be used to infer information about phason elastic constants. We illustrate the theory with explicit computations using icosahedral quasicrystal elastic constants taken from recent density-functional calculations.

I. INTRODUCTION

A number of recent reviews,[1,2] collections of papers,[3,4] and books[5] attest to the explosion of research generated by the experimental discovery[6] of icosahedral quasicrystals. The relative sharpness of the icosahedral diffraction spots initially led to the suggestion[7] that these materials could be described by atomic decorations of the two unit cells embodied in the Ammann tiling,[8] a three-dimensional version of the Penrose tiling.[9] Decorations (based on the known crystallography of large unit-cell conventional crystals) for two broad classes of materials have indeed been proposed.[10,11] Various kinds of disorder must then be invoked to account for the detailed experimental observations. Elser, for example, has argued (using the projection technique[12]) that one can relax the rigid constraints of a literally self-similar Penrose tiling by locally scrambling the tiles. He gave plausible arguments that this could be done in three dimensions (but not for one- or two-dimensional quasiperiodic tilings) in a way which preserved the delta-function character of the peaks, but made pronounced changes in the relative peak intensities.[13] A combination of long-wavelength phason strains and dislocations have been invoked[14] to account for details of the spot positions and the observed peak widths.

The finite linewidths (leading to translational correlation lengths which are at most several hundred angstroms) observed in rapidly quenched materials[15] have stubbornly refused to go away, even in samples grown slowly from the melt.[16] These results lend credence to computer generated "icosahedral glass" models, in which strict long-range icosahedral bond orientational order is imposed on sequentially deposited clusters which need not have infinite range translational order.[17] Although Stephens and Goldman find finite translational correlation lengths with this method,[17] Elser has shown that growth with a modest amount of annealing can sharpen the peaks considerably.[18]

Although we have no strong opinion on this controversy, we think it worthwhile to explore further the consequences of long-range icosahedral translational order, and study in particular the shapes of various Bragg spots.[19] Socolar and Wright[20] have recently examined this question, and postulate a superposition of *uniform* phason strains, arising from growth anisotropies, to account for some of the experimentally observed shapes; the main peak is replicated in slightly different positions to give rise to an apparent anisotropic shape.

Here, we study an alternative mechanism, triggered by *spatially varying* strain fluctuations due to an initially thermalized phason population which has dropped out of equilibrium at an elevated temperature. Similar strains due to quenched random impurities in conventional crystals are well known to lead to anisotropic diffuse scattering, often called Huang scattering.[21] Diffuse scattering is likely to be much weaker than the mechanism proposed in Ref. 20. It is usually down relative to the main peak by an amount proportional to the ratio of a unit-cell size to the translational correlation length. We shall see, however, that there are special enhancement effects peculiar to quasicrystals. Large translational correlation lengths are required to distinguish diffuse scattering from the contribution of a broadened main peak. Experimentalists are probably just at the limits of being able to detect diffuse scattering in quasicrystals.[22]

The theory we construct describes both thermal and quenched diffuse scattering in quasicrystals. If a sample is cooled rapidly, one expects phasons to drop out of equilibrium quickly during the solidification process.[23] The continuum elastic free energy of a well-equilibrated icosahedral crystal with both phonon displacements $\vec{u}(\vec{x})$ and phason displacements $\vec{w}(\vec{x})$ is[24–28]

$$F = F_{\text{phon}}[\vec{u}] + F_{\text{phas}}[\vec{w}] + F_{\text{int}}[\vec{u},\vec{w}] , \tag{1.1}$$

where the pure phonon and phason parts are

$$F_{\text{phon}}[\vec{u}] = \int (\mu u_{ij}^2 + \tfrac{1}{2}\lambda u_{kk}^2) d^3x \tag{1.2}$$

and

$$F_{\text{phas}}[\vec{w}]=\int\left[\frac{m_3}{6}(\partial_i w_j)^2+\frac{m_4}{4\sqrt{5}}\{(\partial_k w_k)^2-\tfrac{4}{3}(\partial_i w_j)^2+[(\tau\partial_1 w_2+\tau^{-1}\partial_2 w_1)^2+\text{cyclic permutations}]\}\right]d^3x\ , \quad (1.3)$$

and the coupling between phonons and phasons is contained in

$$F_{\text{int}}[\vec{u},\vec{w}]=\int\frac{m_5}{2\sqrt{15}}\{[\partial_1 w_1(u_{11}-\tau u_{22}+\tau^{-1}u_{33})+2u_{12}(\tau^{-1}\partial_1 w_2-\tau\partial_2 w_1)]+\text{cyclic permutations}\}d^3x\ . \quad (1.4)$$

The quantities m_3, m_4, and m_5 are elastic constants, λ and μ are the Lamé coefficients, and $u_{ij}=\frac{1}{2}(\partial_i u_j+\partial_j u_i)$. Suppose the phasons drop out of the equilibrium at an elevated temperature T_q during the cooling process. At lower temperatures, the frozen phason displacement field $\vec{w}_q(\vec{x})$ will appear in a quenched random effective free energy

$$F_{\text{eff}}=F_{\text{phon}}[\vec{u}]+F_{\text{int}}[\vec{u},\vec{w}_q]\ , \quad (1.5)$$

where ensemble averages calculated with (1.5) must now be averaged over a *quenched* probability distribution $P_q[\vec{w}_q]$,

$$P_q[\vec{w}_q]\propto\exp\left[-\frac{F_{\text{phas}}[\vec{w}_q]}{k_B T_q}\right]\ . \quad (1.6)$$

Because of the complexity of the quenched quasicrystalline elasticity theory embodied in Eqs. (1.5) and (1.6), we have found it illuminating to compare our results with the simpler case of ordinary Huang scattering from a spatially varying impurity concentration $c(\vec{x})$.[21] In continuum models of Huang scattering, the phonon displacement field $\vec{u}(\vec{x})$ is coupled to quenched random impurity concentration fluctuations $\delta c(\vec{x})=[c(\vec{x})-c_0]/c_0$, where c_0 is the average value of $c(\vec{x})$. Instead of Eqs. (1.5) and (1.6), we now have an effective elastic free energy density[29]

$$F_{\text{eff}}=\int(\mu u_{ij}^2+\tfrac{1}{2}\lambda u_{kk}^2+\gamma u_{kk}\,\delta c)d^3x \quad (1.7)$$

and a quenched probability distribution for $\delta c(\vec{x})$,

$$P_q[\delta c(\vec{x})]\propto\exp\left[-\tfrac{1}{2}\Delta\int d^3x(\delta c)^2/k_B T_q\right]\ , \quad (1.8)$$

where Δ has the dimensions of an elastic constant. Note that we have assumed an isotropic crystal, and that $\delta c(\vec{x})$ couples to the phonon field in much the same way as the quenched phason field $\vec{\nabla}\vec{w}(\vec{x})$ does in quasicrystals.

In Appendix A, we show that the structure factor near a reciprocal-lattice vector $\vec{Q}$ for Huang scattering at temperatures small compared to T_q takes the form

$$S(\vec{q})\propto\{\delta(\vec{k})+Q_i[\mathbf{C}^{-1}(\vec{k})]_{ij}Q_j\}f_0(\vec{Q})\ , \quad (1.9)$$

where $f_0(\vec{Q})$ is analogous to the usual Debye-Waller factor,

$$f_0(\vec{Q})=\exp\left[-\int d^3p Q_i[\mathbf{C}^{-1}(\vec{p})]_{ij}Q_j\right]\ , \quad (1.10)$$

and $\vec{k}=\vec{q}-\vec{Q}$ is assumed small compared to an inverse lattice constant. The 3×3 matrix $\mathbf{C}^{-1}(\vec{k})$ is given in terms of the elastic constants μ and λ and the coupling to the quenched impurities γ by

$$[\mathbf{C}^{-1}(\vec{k})]_{ij}=\frac{\gamma^2 k_B T_q}{\Delta(2\mu+\lambda)^2}\frac{k_i k_j}{k^4}\ . \quad (1.11)$$

As illustrated in Fig. 1, the second, diffuse scattering contribution to $S(\vec{q})$ leads to contours of constant intensity which are pairs of spheres whose common tangent is perpendicular to the radial direction. The intensity increases like k^{-2}, and the *shapes* of the contours around any particular spot are identical. When the anistropic elasticity appropriate to, say, a cubic crystal is incorporated into the theory, one finds that the shape of the contours depends only on the direction of that spot relative to the origin and not on its distance away.[21]

Before quoting the analogous result for icosahedral quasicrystals, we first recall that Bragg spots are most conveniently indexed with *six*-dimensional hypercubic reciprocal-lattice vectors $(\vec{Q}\ \vec{Q}^{\perp})$, where $\vec{Q}$ is the projection of a hypercubical reciprocal-lattice point onto a three-dimensional subspace with icosahedral symmetry.[12,30,31] This subspace is the usual physical space in which the Bragg peaks are actually observed, so $\vec{Q}$ plays a role of a conventional reciprocal-lattice vector. With this notation, the structure function for icosahedral quasicrys-

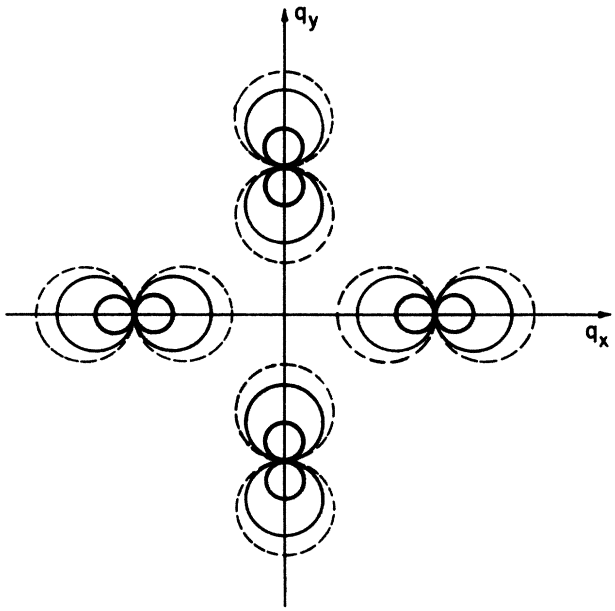

FIG. 1. Constant intensity contours in the (q_x,q_y) plane for Huang scattering from quenched random impurity concentration fluctuations at zero temperature. We have assumed a cubic crystal with isotropic elastic constants for simplicity.

tals near $\vec{q}=\vec{Q}$ has the form (see Secs. II C and III)

$$S(\vec{q}) \propto \left[\delta(\vec{k}) + \tfrac{1}{2}(\vec{Q}\ \vec{Q}^{\perp})\mathbf{C}^{-1}(\vec{k}) \begin{bmatrix} \vec{Q} \\ \vec{Q}^{\perp} \end{bmatrix} \right] \times f_0(\vec{Q},\vec{Q}^{\perp}) \, | \, W(\vec{Q},\vec{Q}^{\perp}) \, |^2 , \quad (1.12)$$

where $\vec{k}=\vec{q}-\vec{Q}$, W is a function characteristic of a particular quasilattice, and f_0 is a Debye-Waller-like factor

$$f_0(\vec{Q},\vec{Q}^{\perp}) = \exp\left[-\int d^3p (\vec{Q}\ \vec{Q}^{\perp})\mathbf{C}^{-1}(\vec{p}) \begin{bmatrix} \vec{Q} \\ \vec{Q}^{\perp} \end{bmatrix} \right] . \quad (1.13)$$

We have again suppressed thermal diffuse scattering for simplicity. The phason-induced quenched diffuse scattering which remains is determined by the 6×6 matrix $\mathbf{C}^{-1}(\vec{k})$, which, like Eq. (1.11), is proportional to $k_B T_q$ and inversely proportional to k^2. It varies with the direction of $\vec{k}$ in a complicated and interesting way which depends on all five quasicrystal elastic constants.

To illustrate our results, we have evaluated Eq. (1.12) using elastic constants extracted from a simple density-functional calculation for quasicrystals.[19,32–34] Density correlations of a dense random packing model of metallic glasses are used as input. As shown in Fig. 2 for diffraction normal to twofold, threefold, and fivefold symmetry axes, the shapes of intensity contours vary kaleidoscopically from spot to spot, even for spots aligned with a particular direction in reciprocal space. We expect a similar rich variation in real experiments, even though the precise magnitudes of the elastic constants obtained in Ref. 32 may not be reliable. If a diverse set of shapes like those in Fig. 2 could be detected and measured with precision, one could work backwards and use the theory presented here to extract information about phason and phonon elastic constants. Then the phason-phonon coupling constant m_5, in particular, is an especially important parameter in interpreting experiments.

At higher temperatures, or if phasons are not quenched, thermal diffuse scattering might become important. For ordinary crystals, contours of constant diffuse scattering intensity sufficiently near a reciprocal-lattice vector $\vec{Q}$ are given by

$$k^2 \propto \sum_{\alpha=1}^{3} \frac{[\vec{Q}\cdot\hat{\varepsilon}_\alpha(\hat{k})]^2}{[v_\alpha(\hat{k})]^2} , \quad (1.14)$$

where $v_\alpha(\hat{k})$ and $\hat{\varepsilon}_\alpha(\hat{k})$ are the three velocities and polarizations of phonons propagating in direction $\hat{k}$. To establish a contact with the subsequent formula for quasicrystals, we note that $\hat{\varepsilon}_\alpha(\hat{k})$ are eigendirections of the 3×3 hydrodynamic elastic matrix $\mathbf{C}(\hat{k})$ [see Eq. (1.11)], while the $[v_\alpha(\hat{k})]^2$ are proportional to its eigenvalues.

In the case of icosahedral quasicrystals, Eq. (1.14) generalizes to

$$k^2 \propto \sum_{\alpha=1}^{6} \frac{[\vec{Q}\cdot\vec{\varepsilon}_\alpha(\hat{k})+\vec{Q}^{\perp}\cdot\vec{\varepsilon}^{\perp}_\alpha(\hat{k})]^2}{[v_\alpha(\hat{k})]^2} , \quad (1.15)$$

where now the hydrodynamic elastic matrix $\mathbf{C}(\hat{k})$ is a

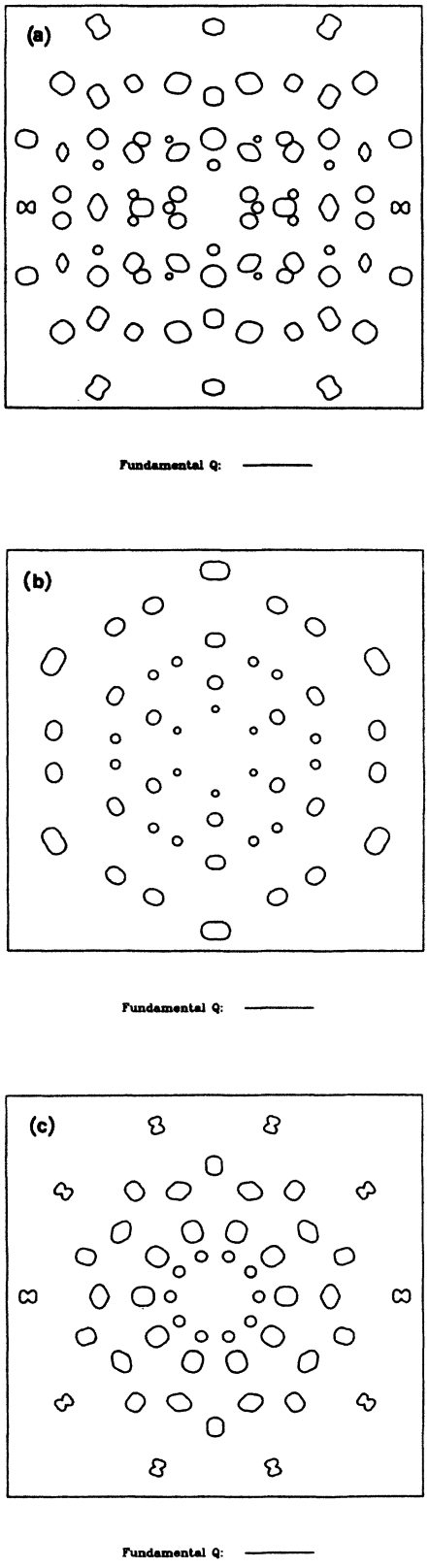

FIG. 2. Contours of constant diffuse scattering in planes perpendicular to (a) twofold, (b) threefold, and (c) fivefold symmetry axes of an icosahedral quasicrystal with quenched random phason displacements at zero temperature. Only contours near Bragg spots with indices 0 or ±1 are shown.

6×6 matrix with six eigendirections and six eigenvalues. If phasons are quenched, the form Eq. (1.15) remains, but the elasticity matrix is replaced by an effective, quenched elasticity matrix whose eigenvalues and eigenvectors do not correspond any more to real propagating modes. It should be noted that phonon and phason degrees of freedom will generally be mixed so that for any given $\alpha=1,\ldots,6$ both $\vec{\varepsilon}_\alpha$ and $\vec{\varepsilon}^{\perp}_\alpha$ will be nonzero.

The theory of diffuse scattering from quasiperiodic crystals, summarized above for icosahedral quasicrystals, is developed in detail in Sec. II. The general theory allows for both thermal diffuse scattering from equilibrated phasons and phonons, and also for the thermal and quenched scattering present when phasons drop out of equilibrium.[35] Characteristic scattering contours similar to Fig. 2 for other circumstances in icosahedral quasicrystals are tabulated in Sec. III. A discussion of ordinary Huang scattering, which parallels the more complicated calculations for incommensurate crystals and quasicrystals, is given in Appendix A. Derivation of some formulas used in Sec. II and III is given in Appendix B. The coordinate systems which we use for icosahedral quasicrystals are specified in Appendix C.

II. SCATTERING FROM DISORDERED QUASIPERIODIC CRYSTALS

A quasiperiodic crystal is a crystal whose three-dimensional Fourier transform (or diffraction pattern) vanishes except on a discrete, but dense set of wave vectors generated by a finite set of basis vectors. This set can be called the reciprocal quasilattice. The smallest number d of wave vectors which generate a reciprocal quasilattice is necessarily greater than three. Quasiperiodic crystals can be further divided into incommensurate crystals and quasicrystals depending on whether or not the rotation symmetry of the reciprocal quasilattice is crystallographic. Since this distinction is not important here, we shall use the term quasicrystal generically.

We want to evaluate the effects of positional disordering on diffraction from quasicrystals. First, we shall introduce necessary notation and a description of the density of a "perfect" quasicrystal. By "perfect," we mean a quasicrystal with δ-function peaks and no diffuse scattering; such a crystal need *not* be generated by literally self-similar inflation rules. We shall also associate an elastic energy with phonon and phason positional disordering. Then, we shall use this elastic energy to derive corrections to the ideal structure factor due to thermalized phonons and thermalized or quenched phasons.

A. Quasicrystal density and its Fourier transform

The set of ideal atomic positions of a quasicrystal can be always represented as a cut through a higher dimensional periodic arrangement of *surfaces*.[36–39] These "atomic" surfaces have dimension equal to the dimension of the higher dimensional space minus the dimension of the physical space and can have complicated topology.[39,40] For example, to obtain the three-dimensional Ammann quasilattice it is necessary to consider a three-dimensional (physical space) cut through a six-dimensional hypercubic periodic lattice whose vertices are covered by identical (three-dimensional) rhombic triacontahedra perpendicular to the cut. The triacontahedra are projections of a six-dimensional unit hypercube onto the three-dimensional complement of the three-dimensional physical subspace.[8,12]

Generally, a quasilattice can be represented by density

$$\rho^{\parallel}(\mathbf{x}^{\parallel})=\rho(\mathbf{x}^{\parallel},\mathbf{x}^{\perp}=\mathbf{0}) , \tag{2.1}$$

where ρ is a periodic density in the hyperspace. Explicitly,

$$\begin{aligned}\rho(\mathbf{x})&=\sum_R \int_{v_c}\delta(\mathbf{x}-\mathbf{R}-\boldsymbol{\xi})\delta^{\parallel}(\boldsymbol{\xi}^{\parallel}-\mathbf{s}^{\parallel}(\boldsymbol{\xi}^{\perp}))d^d\xi\\&=\sum_R \int_{v^{\perp}}\delta^{\parallel}(\mathbf{x}^{\parallel}-\mathbf{R}^{\parallel}-\mathbf{s}^{\parallel}(\boldsymbol{\xi}^{\perp}))\\&\qquad\times\delta^{\perp}(\mathbf{x}^{\perp}-\mathbf{R}^{\perp}-\boldsymbol{\xi}^{\perp})d^{d-3}\xi^{\perp}\\&=\sum_R \delta^{\parallel}(\mathbf{x}^{\parallel}-\mathbf{R}^{\parallel}-\mathbf{s}^{\parallel}(\mathbf{x}^{\perp}-\mathbf{R}^{\perp}))W(\mathbf{x}-\mathbf{R}) ,\end{aligned} \tag{2.2}$$

where $\parallel$ and $\perp$ denote the physical subspace and its orthogonal complement, $\mathbf{R}=(\mathbf{R}^{\parallel},\mathbf{R}^{\perp})$ is a hyperlattice point, v_c denotes unit hypercell (or its volume), and

$$\boldsymbol{\xi}^{\parallel}=\mathbf{s}^{\parallel}(\boldsymbol{\xi}^{\perp}),\quad \boldsymbol{\xi}^{\perp}\in v^{\perp} \tag{2.3}$$

is the equation of the atomic surface decorating the unit hypercells. This surface is defined over the domain ("window") $v^{\perp}$ which can be characterized by the window function

$$W(\mathbf{x})=\begin{cases}1 & \text{if } \mathbf{x}^{\perp}\in v^{\perp}\\ 0 & \text{otherwise.}\end{cases} \tag{2.4}$$

Since there must be a minimal separation between the ideal atomic positions the domain $v^{\perp}$ must be finite.[41] We shall assume here that there is a single atomic surface per unit hypercell. The extension to a more general case is obvious.

As a result of Eqs. (2.1)–(2.4) the quasicrystal density can be written as

$$\rho^{\parallel}(\mathbf{x}^{\parallel})=\sum_{\mathbf{R}}\delta^{\parallel}(\mathbf{x}^{\parallel}-\mathbf{R}^{\parallel}-\mathbf{s}^{\parallel}(-\mathbf{R}^{\perp}))W(-\mathbf{R}^{\perp}) . \tag{2.5}$$

Since there is a one-to-one correspondence between $\mathbf{R}$, $\mathbf{R}^{\perp}$, and $\mathbf{R}^{\parallel}$, a functional dependence on $\mathbf{R}^{\perp}$ can be replaced by a dependence on $\mathbf{R}$ or $\mathbf{R}^{\parallel}$. However, both $\mathbf{s}^{\parallel}$ and W would be highly irregular functions of these variables.

The Fourier transform of the hypercrystal density Eq. (2.2) is

$$\rho(\mathbf{q})\equiv\int\rho(\mathbf{x})e^{-i\mathbf{q}\cdot\mathbf{x}}d^dx=\frac{v^{\perp}}{v_c}\sum_{\mathbf{Q}}\delta(\mathbf{q}-\mathbf{Q})W(\mathbf{Q}) , \tag{2.6}$$

where

$$\begin{aligned}W(\mathbf{q})&=\frac{1}{v^{\perp}}\int_{v_c}e^{-i\mathbf{q}\cdot\boldsymbol{\xi}}\delta^{\parallel}(\mathbf{x}^{\parallel}-\mathbf{s}^{\parallel}(\boldsymbol{\xi}^{\perp}))W(\boldsymbol{\xi}^{\perp})d^d\xi\\&=\frac{1}{v^{\perp}}\int_{v^{\perp}}\exp[-i\mathbf{q}^{\parallel}\cdot\mathbf{s}^{\parallel}(\boldsymbol{\xi}^{\perp})-i\mathbf{q}^{\perp}\cdot\boldsymbol{\xi}^{\perp}]d^{d-3}\xi^{\perp} ,\end{aligned} \tag{2.7}$$

and $\mathbf{Q}=(\mathbf{Q}^{\parallel},\mathbf{Q}^{\perp})$ is a reciprocal hyperlattice vector. A

particular normalization is chosen so that $W(\mathbf{q})$ is dimensionless and equal to unit at $\mathbf{q}=0$. Since the Fourier transform of a cut is equal to a projection of a Fourier transform,[35]

$$\rho^{\parallel}(\mathbf{q})^{\parallel}=\int \rho(\mathbf{q}^{\parallel},\mathbf{q}^{\perp})d^{d-3}q^{\perp} , \tag{2.8}$$

we can immediately write the Fourier transform of the physical, quasicrystal density Eq. (2.5) and obtain a set of weighted delta functions

$$\rho^{\parallel}(\mathbf{q}^{\parallel})=\frac{v^{\perp}}{v_c}\sum_{\mathbf{Q}}\delta^{\parallel}(\mathbf{q}^{\parallel}-\mathbf{Q}^{\parallel})W(\mathbf{Q}) . \tag{2.9}$$

B. Phonon and phason disordering of quasicrystals

A perfect quasilattice can be disordered by allowing displacements of the surface $\mathbf{s}^{\parallel}(\xi^{\perp})$. That is, the surface associated with the hypercell at $\mathbf{R}$ should be replaced by $\mathbf{s}^{\parallel}(\xi^{\perp})+\mathbf{u}^{\parallel}(\mathbf{R},\xi^{\perp})$. In addition, all the singular points $\xi_s^{\perp}$ (that is, the branching points of the surfaces or the boundary of $v^{\perp}$) could be allowed to move. However, only displacements of the surfaces at the intersection with the physical subspace are relevant. Consequently, without lack of generality, we can restrict our attention to rigid surface displacements $\mathbf{u}(\mathbf{R}^{\parallel})$ which are independent of ξ ($\mathbf{u}$ might also carry another index to label different sheets, if $\mathbf{s}^{\parallel}$ is multivalued[41]). That is, $\mathbf{R}+\xi$ in Eq. (2.2) should be replaced by $\mathbf{R}+\xi+\mathbf{u}(\mathbf{R}^{\parallel})$ rather than by $\mathbf{R}+\xi+\mathbf{u}(\mathbf{R},\xi)$, which would be appropriate if we were interested in disordering of the hypercrystal itself. Therefore the quasicrystal is disordered by substituting

$$\mathbf{R}\rightarrow\mathbf{R}+\mathbf{u}(\mathbf{R}^{\parallel}) \tag{2.10}$$

in Eqs. (2.2) and (2.5). It is important to note that disordering of a quasicrystal requires the new, "phason" displacements $\mathbf{u}^{\perp}(\mathbf{R}^{\parallel})$ in addition to the usual, "phonon" displacements $\mathbf{u}^{\parallel}(\mathbf{R}^{\parallel})$. With this substitution, Fourier transform of the hypercrystal density, Eq. (2.6), becomes

$$\rho(\mathbf{q})=v^{\perp}\sum_{\mathbf{R}}e^{-i\mathbf{q}\cdot[\mathbf{R}+\mathbf{u}(\mathbf{R})]}W(\mathbf{q}) , \tag{2.11}$$

while Eq. (2.9) is replaced by

$$\rho^{\parallel}(\mathbf{q}^{\parallel})=v^{\perp}\sum_{\mathbf{R}}\int e^{-i\mathbf{k}\cdot[\mathbf{R}+\mathbf{u}(\mathbf{R})]}W(\mathbf{k})\delta^{\parallel}(\mathbf{k}^{\parallel}-\mathbf{q}^{\parallel})d^{d}k . \tag{2.12}$$

Thermodynamic potential of a quasicrystal does not change under uniform phason or phonon displacements so that nonuniform displacements must be considered. Such displacements can be described by a $d\times 3$ strain matrix, ϵ, which, in the long-wavelength limit, is defined as the gradient of the displacement field,

$$\epsilon=\frac{\partial\mathbf{u}}{\partial\mathbf{x}^{\parallel}} . \tag{2.13}$$

In the block-matrix form, nonzero components of ϵ are the usual, 3×3 symmetric strain matrix

$$\epsilon^{\parallel,\parallel}\equiv\frac{\partial\mathbf{u}^{\parallel}}{\partial\mathbf{x}^{\parallel}} \tag{2.14}$$

and the new, $(d-3)\times 3$ phason strain matrix

$$\epsilon^{\perp,\parallel}\equiv\frac{\partial\mathbf{u}^{\perp}}{\partial\mathbf{x}^{\parallel}} . \tag{2.15}$$

The elastic free energy F of a uniformly strained quasicrystal of volume $V^{\parallel}$ is, to lowest order, quadratic in the strain,[32]

$$F=\tfrac{1}{2}V^{\parallel}(\epsilon:\mathbf{M}:\epsilon)+\cdots$$
$$=\tfrac{1}{2}V^{\parallel}(\epsilon_{\mu,i}M_{\mu,i;\nu,j}\epsilon_{\nu,j})+\cdots , \tag{2.16}$$

and defines the elastic modulus tensor $\mathbf{M}$. That is,

$$\mathbf{M}\equiv\frac{1}{V^{\parallel}}\left[\frac{\partial^2 F}{\partial\epsilon\partial\epsilon}\right]_{\epsilon=0} , \tag{2.17}$$

or, in the component notation,

$$M_{\mu,i;\nu,j}=\frac{1}{V^{\parallel}}\left[\frac{\partial^2 F}{\partial\epsilon_{\mu,i}\partial\epsilon_{\nu,j}}\right]_{\epsilon=0} , \tag{2.18}$$

where indices i and j run over the physical, $\parallel$ coordinates, while μ and ν run over both $\parallel$ and $\perp$ coordinates. The tensor $\mathbf{M}$ can be also written in the block form with the blocks $\mathbf{M}^{\parallel,\parallel;\parallel,\parallel}$, $\mathbf{M}^{\parallel,\parallel;\perp,\parallel}={}^{t}\mathbf{M}^{\perp,\parallel;\parallel,\parallel}$, and $\mathbf{M}^{\perp,\parallel;\perp,\parallel}$. For a slowly varying strain, expression (2.16) for the elastic free energy generalizes to[42]

$$F=\tfrac{1}{2}\int_{V^{\parallel}}\left[\frac{\partial\mathbf{u}}{\partial\mathbf{x}^{\parallel}}:\mathbf{M}:\frac{\partial\mathbf{u}}{\partial\mathbf{x}^{\parallel}}\right]d^3x^{\parallel} , \tag{2.19}$$

or, in terms of the Fourier transforms $\mathbf{u}(\mathbf{p}^{\parallel})$,

$$F=\tfrac{1}{2}\int\mathbf{u}(-\mathbf{p}^{\parallel})\cdot(\mathbf{p}^{\parallel}\cdot\mathbf{M}\cdot\mathbf{p}^{\parallel})\cdot\mathbf{u}(\mathbf{p}^{\parallel})d^3p^{\parallel} . \tag{2.20}$$

The elastic free energy Eq. (2.20) can be also written in terms of phonon, phason, and phonon-phason interaction contributions,

$$F=F_{\text{phon}}[\mathbf{u}^{\parallel}]+F_{\text{phas}}[\mathbf{u}^{\perp}]+F_{\text{int}}[\mathbf{u}^{\parallel},\mathbf{u}^{\perp}] , \tag{2.21}$$

where

$$F_{\text{phon}}[\mathbf{u}^{\parallel}]=\tfrac{1}{2}\int\mathbf{u}^{\parallel}(-\mathbf{p}^{\parallel})\cdot(\mathbf{p}^{\parallel}\cdot\mathbf{M}^{\parallel,\parallel;\parallel,\parallel}\cdot\mathbf{p}^{\parallel})\cdot\mathbf{u}^{\parallel}(\mathbf{p}^{\parallel})d^3p^{\parallel} , \tag{2.22}$$

$$F_{\text{phas}}[\mathbf{u}^{\perp}]=\tfrac{1}{2}\int\mathbf{u}^{\perp}(-\mathbf{p}^{\parallel})\cdot(\mathbf{p}^{\parallel}\cdot\mathbf{M}^{\perp,\parallel;\perp,\parallel}\cdot\mathbf{p}^{\parallel})\cdot\mathbf{u}^{\perp}(\mathbf{p}^{\parallel})d^3p^{\parallel} , \tag{2.23}$$

and

$$F_{\text{int}}[\mathbf{u}^{\parallel},\mathbf{u}^{\perp}]=\int\mathbf{u}^{\perp}(-\mathbf{p}^{\parallel})\cdot(\mathbf{p}^{\parallel}\cdot\mathbf{M}^{\perp,\parallel;\parallel,\parallel}\cdot\mathbf{p}^{\parallel})\cdot\mathbf{u}^{\parallel}(\mathbf{p}^{\parallel})d^3p^{\parallel} . \tag{2.24}$$

These elastic free energies will determine probability distributions over which functionals of phonon and phason displacement fields will be averaged.

C. Structure factor of disordered quasicrystals

From Eq. (2.9) we can immediately obtain the structure factor for the perfect quasilattice

$$S^{\parallel}(\mathbf{q}^{\parallel})\equiv\frac{|\rho^{\parallel}(\mathbf{q}^{\parallel})|^2}{N^{\parallel}}=\frac{v^{\perp}}{v_c}\sum_{\mathbf{Q}}\delta^{\parallel}(\mathbf{q}^{\parallel}-\mathbf{Q}^{\parallel})\,|\,W(\mathbf{Q})\,|^2\,, \tag{2.25}$$

where we used a generalization of the usual substitution for the square of the delta function, proved in Appendix B, and where $N^{\parallel}$ is the number of the quasilattice points. $N^{\parallel}$ equals the number of the surfaces $\mathbf{s}^{\parallel}$ cut by the physical subspace.

In order to calculate structure factor of a disordered quasicrystal, the density given by Eq. (2.12) rather than by Eq. (2.9) must be substituted into Eq. (2.25). Moreover, the resulting structure factor corresponds to a particular realization of disorder $\mathbf{u}(\mathbf{R})$ so it has to be averaged over a distribution $P[\mathbf{u}]$ of displacements. Therefore we can write the structure factor, averaged over a distribution of $\mathbf{u}$, as

$$S^{\parallel}(\mathbf{q}^{\parallel})=\frac{v^{\perp 2}}{N^{\parallel}}\sum_{\mathbf{R}_1\mathbf{R}_2}\int\int e^{i\mathbf{k}_2\cdot\mathbf{R}_2-i\mathbf{k}_1\cdot\mathbf{R}_1}fW(\mathbf{k}_1)W^*(\mathbf{k}_2)\delta^{\parallel}(\mathbf{q}^{\parallel}-\mathbf{k}_1^{\parallel})\delta^{\parallel}(\mathbf{q}^{\parallel}-\mathbf{k}_2^{\parallel})d^dk_1\,d^dk_2\,, \tag{2.26}$$

where f denotes the average

$$f\equiv\int\mathcal{D}[u]e^{i\mathbf{k}_2\cdot\mathbf{u}(\mathbf{R}_2)-i\mathbf{k}_i\cdot\mathbf{u}(\mathbf{R}_1)}P[\mathbf{u}]\,. \tag{2.27}$$

As we shall see below, independently of whether phasons are thermalized or quenched, the distribution $P[\mathbf{u}]$ will be Gaussian,

$$P[\mathbf{u}]\propto\exp\left[-\tfrac{1}{2}\int\mathbf{u}(-\mathbf{p}^{\parallel})\cdot\mathbf{C}(\mathbf{p}^{\parallel})\cdot\mathbf{u}(\mathbf{p}^{\parallel})d^3p^{\parallel}\right]\,, \tag{2.28}$$

where $\mathbf{u}(\mathbf{p}^{\parallel})$ is a Fourier component of $\mathbf{u}$,

$$\mathbf{u}(\mathbf{R}^{\parallel})=\int e^{i\mathbf{p}^{\parallel}\cdot\mathbf{R}^{\parallel}}\mathbf{u}(\mathbf{p}^{\parallel})d^3p^{\parallel}\,, \tag{2.29}$$

and $d\times d$ matrix $\mathbf{C}(\mathbf{p}^{\parallel})$, which is even under $\mathbf{p}^{\parallel}\rightarrow-\mathbf{p}^{\parallel}$, Hermitian, and positive definite, is related to the elastic modulus tensor $\mathbf{M}$. Then, following the derivation given in Appendix B, the structure factor can be written as an expansion,

$$S^{\parallel}(\mathbf{q}^{\parallel})=S_0^{\parallel}(\mathbf{q}^{\parallel})+S_1^{\parallel}(\mathbf{q}^{\parallel})+\cdots\,, \tag{2.30}$$

whose first two terms are the Bragg scattering

$$S_0^{\parallel}(\mathbf{q}^{\parallel})=\frac{v^{\perp}}{v_c}(2\pi)^{2d-3}\sum_{\mathbf{Q}}\delta^{\parallel}(\mathbf{q}^{\parallel}-\mathbf{Q}^{\parallel})\,|\,W(\mathbf{Q})\,|^2f_0(\mathbf{Q}) \tag{2.31}$$

and the lowest-order diffuse scattering

$$S_1^{\parallel}(\mathbf{q}^{\parallel})=\frac{v^{\perp}}{2v_c}(2\pi)^{2d-3}\times\sum_{\mathbf{Q}}\left[(\mathbf{q}^{\parallel}\mathbf{Q}^{\perp})\cdot\mathbf{C}^{-1}(\mathbf{q}^{\parallel}-\mathbf{Q}^{\parallel})\cdot\begin{bmatrix}\mathbf{q}^{\parallel}\\ \mathbf{Q}^{\perp}\end{bmatrix}\right]\times|\,W(\mathbf{q}^{\parallel},\mathbf{Q}^{\perp})\,|^2f_0(\mathbf{q}^{\parallel},\mathbf{Q}^{\perp})\,, \tag{2.32}$$

where

$$f_0(\mathbf{q})=\exp\left[-\tfrac{1}{2}\int\mathbf{q}\cdot\mathbf{C}^{-1}(\mathbf{p}^{\parallel})\cdot\mathbf{q}\,d^3p^{\parallel}\right] \tag{2.33}$$

is analogous to the Debye-Waller factor.

As can be seen from formulas (2.30)–(2.33), near a particular quasilattice point $\mathbf{Q}$ the structure factor can be written as

$$S^{\parallel}(\mathbf{Q}^{\parallel}+\mathbf{k}^{\parallel})\approx\frac{v^{\perp}}{v_c}(2\pi)^{2d-3}[\delta^{\parallel}(\mathbf{k}^{\parallel})+\tfrac{1}{2}\mathbf{Q}\cdot\mathbf{C}^{-1}(\mathbf{k}^{\parallel})\cdot\mathbf{Q}]\times|\,W(\mathbf{Q})\,|^2f_0(\mathbf{Q})\,. \tag{2.34}$$

This is a generalization of the formula (1.12) quoted in the introductory section. It follows from the second term in the above equation that sufficiently near a Bragg spot, contours of constant diffuse scattering are given by

$$\mathbf{Q}\cdot\mathbf{C}^{-1}(\mathbf{k}^{\parallel})\cdot\mathbf{Q}=\text{const}\,. \tag{2.35}$$

It will be shown in the last part of this section that $\mathbf{C}(\mathbf{k}^{\parallel})$ is quadratic in $\mathbf{k}^{\parallel}$. Therefore Eq. (2.35) can be written more explicitly as

$$|\,\mathbf{k}^{\parallel}\,|^2=\text{const}\times\sum_{\alpha=1}^{d}\frac{[\mathbf{Q}\cdot\hat{\boldsymbol{\varepsilon}}_{\alpha}(\hat{\mathbf{k}}^{\parallel})]^2}{[v_{\alpha}(\hat{\mathbf{k}}^{\parallel})]^2}=\text{const}\times\sum_{\alpha=1}^{d}\frac{[\mathbf{Q}^{\parallel}\cdot\boldsymbol{\varepsilon}_{\alpha}^{\parallel}(\hat{\mathbf{k}}^{\parallel})+\mathbf{Q}^{\perp}\cdot\boldsymbol{\varepsilon}_{\alpha}^{\perp}(\hat{\mathbf{k}}^{\parallel})]^2}{[v_{\alpha}(\hat{\mathbf{k}}^{\parallel})]^2}\,, \tag{2.36}$$

where $\hat{\boldsymbol{\varepsilon}}_{\alpha}(\hat{\mathbf{k}}^{\parallel})$ denotes the d unit eigenvectors of $\mathbf{C}(\hat{\mathbf{k}}^{\parallel})$ while $[v_{\alpha}(\hat{\mathbf{k}}^{\parallel})]^2$ are proportional to the corresponding d positive eigenvalues of $\mathbf{C}(\hat{\mathbf{k}}^{\parallel})$. Clearly, for a very large $\mathbf{Q}^{\perp}$ and relatively fixed $\mathbf{Q}^{\parallel}$, the shape of the contours will be dominated by the $\mathbf{Q}^{\perp}$ contribution. Equation (1.15) quoted in the Introduction is a special case of the above formula.

It should be also noted, that unlike for ordinary crystals, even for a fixed direction $\hat{\mathbf{Q}}^{\parallel}$, the shape of the contours depends also on the magnitude $|\,\mathbf{Q}^{\parallel}\,|$. The reason is that spots with collinear $\mathbf{Q}^{\parallel}$ need not have collinear $\mathbf{Q}$. For example, in icosahedral quasicrystals there are diffraction spots $\mathbf{Q}^{\parallel}$ which are collinear and in proportion to the golden mean. Such spots, however, do not have collinear $\mathbf{Q}$'s and, consequently, they should have different diffuse shapes.[27]

The $d\times d$ matrix $\mathbf{C}(\mathbf{p}^{\parallel})$ which determines the probability distribution Eq. (2.28) can be related to the elastic modulus tensor of the quasicrystal. If phasons, as well as phonons, are thermalized, then the distribution function

Eq. (2.28) is simply the Boltzmann distribution associated with the elastic energy given by Eq. (2.20). Consequently the matrix $\mathbf{C}(\mathbf{p}^{\parallel})$ in Eq. (2.28) is in this case

$$C_{\mu,\nu}(\mathbf{p}^{\parallel}) \equiv \frac{1}{k_B T}(p_i^{\parallel} M_{\mu,i;\nu,j} p_j^{\parallel}) , \tag{2.37}$$

where T is temperature and k_B is the Boltzmann constant. We shall call this matrix the hydrodynamic matrix. It is easy to verify from corresponding hydrodynamic equations that eigenvalues of $\mathbf{C}(\mathbf{p}^{\parallel})$ are proportional to the squares of velocities of the eigenmodes associated with the wave vector $\mathbf{p}^{\parallel}$.

If, however, phasons drop out of thermal equilibrium at a temperature T_q, then at a lower temperature T, phonons will equilibrate in the presence of a quenched phason displacement field $\mathbf{u}_q^{\perp}$. Therefore, the average in Eq. (2.27) will require two steps. First, the ensemble average over phonons must be completed using the effective Boltzmann distribution

$$P_{\text{eff}}[\mathbf{u}^{\parallel}] \propto \exp\left[-\frac{F_{\text{eff}}}{k_B T}\right] , \tag{2.38}$$

where the quenched random effective free energy F_{eff} is

$$F_{\text{eff}} = F_{\text{phon}}[\mathbf{u}^{\parallel}(\mathbf{p}^{\parallel})] + F_{\text{int}}[\mathbf{u}^{\parallel}(\mathbf{p}^{\parallel}), \mathbf{u}_q^{\perp}(\mathbf{p}^{\parallel})] , \tag{2.39}$$

and where F_{phon} and F_{int} are given in Eqs. (2.22) and (2.24). Second, this ensemble average must be averaged over a quenched probability distribution $P_q[\mathbf{u}_q^{\perp}]$,

$$P_q[\mathbf{u}_q^{\perp}] \propto \exp\left[-\frac{F_{\text{phas}}[\mathbf{u}_q^{\perp}(\mathbf{p}^{\parallel})]}{k_B T_q}\right] , \tag{2.40}$$

where F_{phas} is given in Eq. (2.23). The average over the phason distribution can be viewed as an average over an ensemble of different samples, or as "self-averaging" in a single, but very large sample.

It can be easily verified, using the results of Appendix B, that the two averaging steps with Eqs. (2.38) and (2.40) are equivalent to a single step as in Eq. (2.28) with $\mathbf{C}^{\parallel,\parallel}$, $\mathbf{C}^{\perp,\parallel}$, and $\mathbf{C}^{\parallel,\perp}$ blocks of the matrix C given by Eq. (2.37) and the $\mathbf{C}^{\perp,\perp}$ block given by

$$\mathbf{C}^{\perp,\perp}(\mathbf{p}^{\parallel}) = \mathbf{C}_q^{\perp,\perp}(\mathbf{p}^{\parallel}) + \mathbf{C}^{\perp,\parallel}(\mathbf{p}^{\parallel}) \cdot [\mathbf{C}^{\parallel,\parallel}(\mathbf{p}^{\parallel})]^{-1} \cdot \mathbf{C}^{\parallel,\perp}(\mathbf{p}^{\parallel}) , \tag{2.41}$$

where

$$[\mathbf{C}_q^{\perp,\perp}(\mathbf{p}^{\parallel})]_{\alpha\beta} = \frac{1}{k_B T_q} p_i^{\parallel} M^{\perp,\parallel;\perp,\parallel}_{\alpha,i;\beta,j} p_j^{\parallel} . \tag{2.42}$$

The last term in Eq. (2.41) compensates for a spurious term which would arise from averaging over the phonon field. It should be emphasized that elastic modulus tensor $\mathbf{M}$ will generally depend on temperature so its values at T and T_q should be used in Eqs. (2.37) and (2.42), respectively.

III. RESULTS FOR ICOSAHEDRAL QUASICRYSTALS

A density $\rho^{\parallel}(\mathbf{x}^{\parallel})$ whose diffraction pattern consists of Bragg peaks which can be completely indexed with the six vertex vectors of an icosahedron, can be always viewed as a cut through a six-dimensional hypercubic crystal.[39] The orientation of the icosahedral group with respect to the coordinate axes in the physical and the complementary spaces can be specified by specifying the orientation of the projections (components) of the six orthonormal vectors, which span the six-dimensional space and which are assumed perpendicular to the five faces of the hypercubic unit cell. With the specific orientation given in Appendix C, and using group theory, it can be shown that the hydrodynamic matrix $\mathbf{C}(\mathbf{p}^{\parallel})$ can be represented as a sum of five basic matrices:[23–27]

$$\mathbf{C}^{\parallel,\parallel}(\mathbf{p}^{\parallel}) = c_1 \hat{\mathbf{C}}_1^{\parallel,\parallel}(\mathbf{p}^{\parallel}) + c_2 \hat{\mathbf{C}}_2^{\parallel,\parallel}(\mathbf{p}^{\parallel}) , \tag{3.1}$$

$$\mathbf{C}^{\perp,\perp}(p^{\parallel}) = c_3 \hat{\mathbf{C}}_3^{\perp,\perp}(\mathbf{p}^{\parallel}) + c_4 \hat{\mathbf{C}}_4^{\perp,\perp}(\mathbf{p}^{\parallel}) , \tag{3.2}$$

and

$$\mathbf{C}^{\parallel,\perp}(\mathbf{p}^{\parallel}) = {}^t\mathbf{C}^{\perp,\parallel}(\mathbf{p}^{\parallel}) = c_5 \hat{\mathbf{C}}^{\parallel,\perp}(\mathbf{p}^{\parallel}) , \tag{3.3}$$

where prefix t denotes transpose, and[43]

$$[\hat{\mathbf{C}}_1^{\parallel,\parallel}(\mathbf{p}^{\parallel})]_{ij} = \frac{1}{2\sqrt{6}}(p_i^{\parallel} p_j^{\parallel} + |\mathbf{p}^{\parallel}|^2 \delta_{ij}) , \tag{3.4}$$

$$[\hat{\mathbf{C}}_2^{\parallel,\parallel}(\mathbf{p}^{\parallel})]_{ij} = \frac{1}{2\sqrt{30}}(3p_i^{\parallel} p_j^{\parallel} - |\mathbf{p}^{\parallel}|^2 \delta_{ij}) , \tag{3.5}$$

$$[\hat{\mathbf{C}}_3^{\perp,\perp}(\mathbf{p}^{\parallel})]_{ij} = \tfrac{1}{3}|\mathbf{p}^{\parallel}|^2 \delta_{ij} , \tag{3.6}$$

$$\hat{\mathbf{C}}_4^{\perp,\perp}(\mathbf{p}^{\parallel}) = \frac{-1}{2\sqrt{5}} \begin{bmatrix} \tfrac{1}{3}|\mathbf{p}^{\parallel}|^2 + \tau^{-1} p_2^{\parallel 2} - \tau p_3^{\parallel 2} & -2p_1^{\parallel} p_2^{\parallel} & -2p_1^{\parallel} p_3^{\parallel} \\ -2p_2^{\parallel} p_1^{\parallel} & \tfrac{1}{3}|\mathbf{p}^{\parallel}|^2 + \tau^{-1} p_3^{\parallel 2} - \tau p_1^{\parallel 2} & -2p_2^{\parallel} p_3^{\parallel} \\ -2p_3^{\parallel} p_1^{\parallel} & -2p_3^{\parallel} p_2^{\parallel} & \tfrac{1}{3}|\mathbf{p}^{\parallel}|^2 + \tau^{-1} p_1^{\parallel 2} - \tau p_2^{\parallel 2} \end{bmatrix} , \tag{3.7}$$

and

$$\hat{\mathbf{C}}_5^{\parallel,\perp}(\mathbf{p}^{\parallel}) = \frac{1}{\sqrt{60}} \begin{bmatrix} p_1^{\parallel 2} - \tau p_2^{\parallel 2} + \tau^{-1} p_3^{\parallel 2} & 2\tau^{-1} p_1^{\parallel} p_2^{\parallel} & -2\tau p_1^{\parallel} p_3^{\parallel} \\ -2\tau p_2^{\parallel} p_1^{\parallel} & p_2^{\parallel 2} - \tau p_3^{\parallel 2} + \tau^{-1} p_1^{\parallel 2} & 2\tau^{-1} p_2^{\parallel} p_3^{\parallel} \\ 2\tau^{-1} p_3^{\parallel} p_1^{\parallel} & -2\tau p_3^{\parallel} p_2^{\parallel} & p_3^{\parallel 2} - \tau p_1^{\parallel 2} + \tau^{-1} p_2^{\parallel 2} \end{bmatrix} . \tag{3.8}$$

The coefficients c_i are simply related to the five independent elastic moduli[27] m_i by

$$c_i = \frac{m_i}{k_B T}, \quad i = 1, \ldots, 5 . \tag{3.9}$$

In order to obtain equations quoted in the Introduction it is necessary to change the notation according to $(\mathbf{u}^{\parallel}, \mathbf{u}^{\perp}) \leftrightarrow (\vec{u}, \vec{w})$, $\mathbf{x}^{\parallel} \leftrightarrow \vec{x}$, $\mathbf{p}^{\parallel} \leftrightarrow \vec{p}$, $\mathbf{k}^{\parallel} \leftrightarrow \vec{k}$, $(\boldsymbol{\varepsilon}^{\parallel}, \boldsymbol{\varepsilon}^{\perp}) \leftrightarrow (\vec{\varepsilon}, \vec{\varepsilon}^{\perp})$, and $(\mathbf{Q}^{\parallel}\ \mathbf{Q}^{\perp}) \leftrightarrow (\vec{Q}\ \vec{Q}^{\perp})$. Also, by projecting longitudinal and transverse components out of Eqs. (3.4) and (3.5), it is possible to verify that the Lammé coefficients λ and μ which appear in Eq. (1.2) are related to m_1 and m_2 by $m_1 = (2\mu + \frac{1}{2}\lambda)\sqrt{6}$ and $m_2 = \lambda(\frac{15}{2})^{1/2}$.

A metastable quasicrystalline icosahedral structure[33] and its elastic modulus tensor[19,32] $\mathbf{M}$ have been previously investigated for hypothetical icosahedral quasicrystals using a density-functional theory. This theory is based on an expansion of the interaction part of the Helmholtz thermodynamic functional around a reference, supercooled liquid state. The expansion is usually truncated at the second order so that the information about interparticle interactions is manifested only through the direct pair correlation function in the reference liquid state.

Structure factor of a reference supercooled liquid at its glass temperature T_g can be identified with structure factor of the glass at $T \leq T_g$. On the other hand, structure factor of metallic glasses, such as amorphous iron and nickel, can be successfully represented by dense random packing models.[44] As a result, the coefficients c_i of the corresponding icosahedral quasicrystal[33] at $T = T_g$ were found to be[32]

$$\begin{aligned} c_1 &\approx 1.6 \times 10^3 , \\ c_2 &\approx 2.2 \times 10^3 , \\ c_3 &\approx 4.9 \times 10^2 , \\ c_4 &\approx -5.9 \times 10^1 , \\ c_5 &\approx 9.2 \times 10^1 \end{aligned} \tag{3.10}$$

in units of the average quasicrystal density ($=v^{\perp}/v_c$).

The interaction coefficient c_5 is particularly important for diffuse scattering. Sufficiently large c_5 destabilizes[32] matrix $\mathbf{C}$. Therefore, even for elastically stable quasicrystals, a large coefficient c_5 could lead to some anomalously small eigenvalues $v_\alpha(\hat{\mathbf{k}})$ and, consequently, to anomalously large diffuse scattering. Similar anomalously large scattering could be also observed in certain directions around wave vectors $\mathbf{Q}^{\parallel}$ which have a large $\mathbf{Q}^{\perp}$ component, provided corresponding contribution to the Debye-Waller factor,

$$\tfrac{1}{3}\int \mathrm{tr}[\mathbf{C}^{-1}(\hat{\mathbf{p}}^{\parallel})]^{\perp\perp} d^2\hat{p}^{\parallel} = \tfrac{1}{3}\int \sum_{\alpha=1}^{6} \frac{[\boldsymbol{\varepsilon}_\alpha^{\perp}(\hat{\mathbf{p}}^{\parallel})]^2}{[v_\alpha(\hat{\mathbf{p}}^{\parallel})]^2} d^2\hat{p}^{\parallel} , \tag{3.11}$$

is sufficiently small. Note that for icosahedral quasicrystals the Debye-Waller factor Eq. (2.33) can be written as

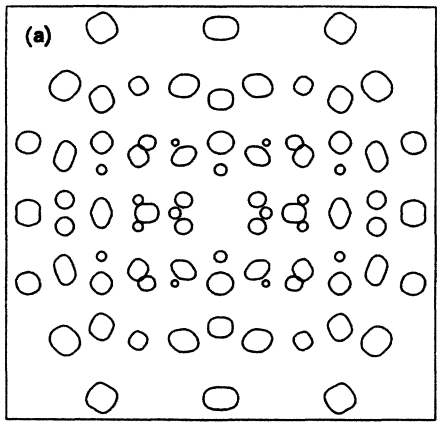

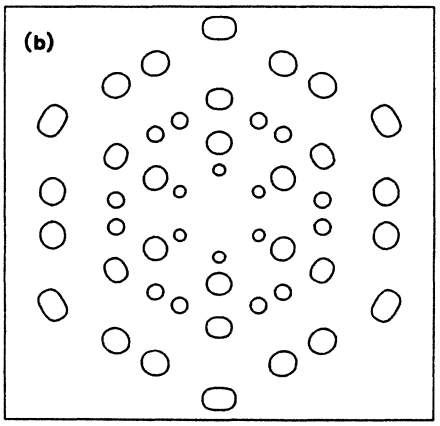

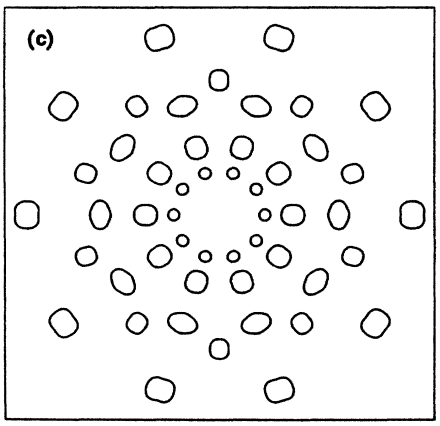

FIG. 3. Same as in Fig. 2, except at finite temperature $T = \frac{1}{3}T_q$.

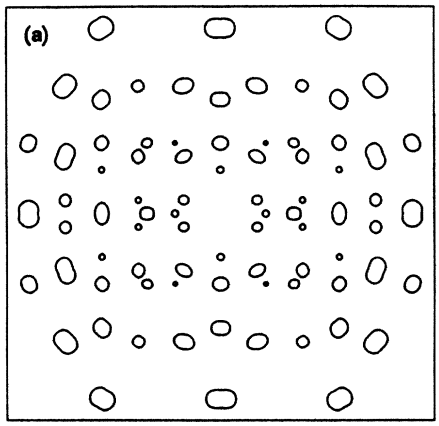

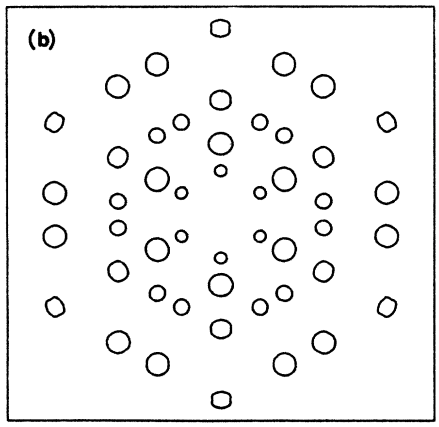

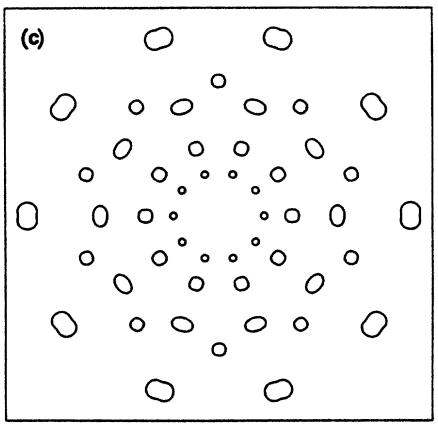

FIG. 4. Same as in Fig. 3, except that phasons are assumed thermalized.

$$f_0(\mathbf{Q})=\exp\left[-\tfrac{1}{2}\int\left[|\mathbf{Q}^{\parallel}|^2\frac{\mathrm{tr}[\mathbf{C}^{-1}(\mathbf{p}^{\parallel})]^{\parallel,\parallel}}{3}+|\mathbf{Q}^{\perp}|^2\frac{\mathrm{tr}[\mathbf{C}^{-1}(\mathbf{p}^{\parallel})]^{\perp,\perp}}{3}\right]d^3p^{\parallel}\right]. \tag{3.12}$$

With the above values for the coefficients c_i, we calculated contours of constant diffuse scattering using Eq. (2.36) or its equivalent Eq. (1.15). In Fig. 2 we showed contours in the planes perpendicular to the twofold, threefold, and fivefold symmetry axes for quenched phasons in the limit $T=0$. We assumed that the phason quench temperature T_q is approximately equal to the melting temperature of the stable crystal, $T_q \approx T_m$, and that $T_m \approx 3T_g$.[45] It was also assumed that $m_5(T_m) \approx m_5(T_g)$ and that the ratios of the moduli m_i, $i=1,2,3,4$ are approximately the same at $T=0$ and $T=T_g$.

In Fig. 3 we also show the results for quenched phasons, but now we take $T=T_g$. Finally, in Fig. 4 we show analogous results for the case when both phonons and phasons are thermalized at $T=T_g$.

IV. CONCLUSIONS

The effect of phonon and phason disordering on scattering from quasicrystals was examined in this paper. An explicit formula was derived to relate the Debye-Waller factor of a quasicrystal to its elastic moduli [Eq. (2.33) and Eqs. (2.37) and (2.42)]. Lowest order diffuse scattering from quasicrystals has been also described explicitly in terms of the elastic moduli [Eqs. (2.32) and (2.36) and Eqs. (2.37) and (2.42)].

The derived general formulas were applied to a specific case of icosahedral quasicrystals. Representative contours of constant diffuse scattering were calculated for cases of quenched and thermalized phasons. Two main observations could be made: shape of the contours is much more complicated than what would be possible in the case of ordinary crystals (or isotropic solids); unlike ordinary simple crystals, shape of the contours varies even among the collinear Bragg spots. These are signatures of phason degrees of freedom. Moreover, for large $\mathbf{Q}^{\perp}$ both the Debye-Waller factor and the diffuse scattering contours are dominated by $\mathbf{Q}^{\perp}$ components. Therefore these are the characteristic features which can experimentally identify quasicrystals.

A careful experimental measurement of diffuse scattering in quasicrystals might be the best way to evaluate their elastic moduli. Such measurements should be done as a function of temperature (so that the quenched, temperature-independent contribution can be isolated) and as a function of quench rates (so that the temperature-dependent contribution can be isolated).

ACKNOWLEDGMENTS

We acknowledge several useful discussions with P. Horn, S. Moss, F. Spaepen, and D. Turnbull. One of us (M.V.J.) would also like to thank for hospitality Istituto

per l'Interscambio Scientifico (Torino, Italy), and the staff of Villa Gualino, where this work was completed. This work was supported in part by the National Science Foundation (NSF) through the Harvard University Materials Research Laboratory and Grant No. DMR-85-14638.

APPENDIX A: CONTINUUM ELASTIC THEORY OF HUANG SCATTERING

In this appendix, we review the continuum elastic theory of Huang scattering from a fluctuating impurity concentration $\delta c(\vec{x})$. Although the results are not new, they illustrate the notation and calculational techniques employed for quasicrystals in the body of this paper and in Appendix B.

As discussed in the Introduction, we consider an isotropic elastic free energy with a linear coupling of the local dilation $u_{kk}(\vec{x})=\vec{\nabla}\cdot\vec{u}(\vec{x})$ to $\delta c(\vec{x})$,

$$F_{\text{eff}}=\tfrac{1}{2}\int d^3x(2\mu u_{ij}^2+\lambda u_{kk}^2+2\gamma\,\delta c\,u_{kk})\ . \tag{A1}$$

We assume for simplicity an isotropic crystal in a periodic box of volume V, and make the Fourier decomposition,

$$\vec{u}(\vec{x})=\frac{1}{V}\sum_{\vec{q}} e^{-i\vec{q}\cdot\vec{x}}\vec{u}(\vec{q})\ , \tag{A2}$$

where

$$\vec{u}(\vec{q})=\int_V d^3x\, e^{-i\vec{q}\cdot\vec{x}}\vec{u}(\vec{x})\ . \tag{A3}$$

Upon passing to Fourier variables for $\delta c(\vec{x})$ as well, the free energy becomes

$$F_{\text{eff}}=F_0+\frac{i\gamma}{V}\sum_{\vec{q}}[\vec{q}\cdot\vec{u}(\vec{q})]\delta c(-\vec{q})\ , \tag{A4}$$

where F_0 can be written in terms of longitudinal and transverse projection operators in reciprocal space as

$$F_0=\frac{1}{2V}\sum_{\vec{q}} q^2\left[\mu\left[\delta_{ij}-\frac{q_iq_j}{q^2}\right]+(2\mu+\lambda)\frac{q_iq_j}{q^2}\right]\times u_i(\vec{q})u_j(-\vec{q})\ . \tag{A5}$$

To calculate the thermodynamic average of a quantity A using (A4) for a fixed impurity distribution $\delta c(\vec{x})$, we must first carry out a functional integral over the displacement field $\vec{u}(\vec{x})$,

$$\langle A\rangle=\frac{\int\mathcal{D}[\vec{u}(\vec{x})]A\exp(-F_{\text{eff}}/k_BT)}{\int\mathcal{D}[\vec{u}(\vec{x})]\exp(-F_{\text{eff}}/k_BT)}\ , \tag{A6}$$

where the square brackets denote the thermodynamic average. We must then average over the quenched impurity field. When expressed in Fourier-transformed variables, the quenched probability distribution of Eq. (1.8) is

$$P_q[\delta c]\propto\exp\left[-\frac{\Delta}{2k_BT_q}\frac{1}{V}\sum_{\vec{q}}|\delta c(\vec{q})|^2\right]\ . \tag{A7}$$

Denoting impurity averages by an overbar, we can average over both displacements and the impurity distribution (A7) as follows:

$$\overline{\langle A\rangle}=\frac{\int\mathcal{D}[\delta c(\vec{x})]\langle A\rangle P_q(\delta c)}{\int\mathcal{D}[\delta c(\vec{x})]P_q(\delta c)}\ . \tag{A8}$$

We now investigate fluctuations in the particle density $\rho(\vec{x})$,

$$\rho(\vec{x})=\sum_{\vec{R}}\delta(\vec{x}-\vec{R}-\vec{u}(\vec{R}))\ , \tag{A9}$$

where the sum runs over the sites $\{\vec{R}\}$ of a regular lattice with reciprocal lattice vectors $\{\vec{Q}\}$. The Fourier transformed density reads

$$\rho(\vec{q})=\sum_{\vec{R}} e^{i\vec{q}\cdot[\vec{R}+\vec{u}(\vec{R})]}=\sum_{\vec{R}} e^{i\vec{k}\cdot\vec{R}}e^{i\vec{q}\cdot\vec{u}(\vec{R})}\ , \tag{A10}$$

where we have set $\vec{q}=\vec{Q}+\vec{k}$. The quantity measured in diffraction experiments is the structure factor $S(\vec{q})$,

$$S(\vec{q})=\langle|\rho(\vec{q})|^2\rangle/N=\sum_{\vec{R}} e^{i\vec{k}\cdot\vec{R}}\overline{\langle e^{i\vec{q}\cdot[\vec{u}(\vec{R})-\vec{u}(\vec{0})]}\rangle}\ . \tag{A11}$$

We shall be interested here in the behavior of $S(\vec{q})$ for $\vec{q}$ near a particular reciprocal-lattice vector $\vec{Q}$, and will therefore set $\vec{q}=\vec{Q}$ inside the averages of Eq. (A11). We can also replace the sum over $\vec{R}$ by an integral over $\vec{x}$ in this limit.

The thermodynamic part of the average in (A11) can be simplified as follows:

$$\begin{aligned}\langle e^{i\vec{Q}\cdot[\vec{u}(\vec{x})-\vec{u}(\vec{0})]}\rangle&=\frac{\left\langle\exp\left[i\vec{Q}\cdot[\vec{u}(\vec{x})-\vec{u}(\vec{0})]-\frac{\gamma}{k_BT}\int d^3x'u_{kk}(\vec{x}')\delta c(\vec{x}')\right]\right\rangle_0}{\left\langle\exp\left[\frac{-\gamma}{k_BT}\int d^3x'u_{kk}(\vec{x}')\delta c(\vec{x}')\right]\right\rangle_0}\\&=\exp\left[-\tfrac{1}{2}Q_iQ_j\langle[u_i(\vec{x})-u_i(\vec{0})][u_j(\vec{x})-u_j(\vec{0})]\rangle_0\right.\\&\quad\left.-\frac{\gamma}{k_BT}Q_j\int d^3x'\,\delta c(x')\langle u_{kk}(\vec{x}')[u_j(\vec{x})-u_j(\vec{0})]\rangle_0\right]\ ,\end{aligned} \tag{A12}$$

where $\langle\ \rangle_0$ denotes an average with respect to the free energy F_0 and we have used standard properties of Gaussian integrals. The two exponentiated thermal averages in (A12) are readily evaluated using Fourier variables and the free energy (A5):

$$\langle [u_i(\vec{x})-u_i(\vec{0})][u_j(\vec{x})-u_j(\vec{0})]\rangle_0 \equiv U_{ij}(\vec{x}) = \frac{2k_BT}{V}\sum_{\vec{p}}\frac{1}{p^2}(1-e^{i\vec{p}\cdot\vec{x}})\left[\frac{1}{\mu}\left[\delta_{ij}-\frac{p_ip_j}{p^2}\right]+\frac{1}{2\mu+\lambda}\frac{p_ip_j}{p^2}\right], \tag{A13}$$

$$\langle u_{kk}(\vec{x}')[u_j(\vec{x})-u_j(\vec{0})]\rangle_0 \equiv V_j(\vec{x}',\vec{x}) = -\frac{ik_BT}{2\mu+\lambda}\frac{1}{V}\sum_{\vec{p}}\frac{p_j}{p^2}(e^{i\vec{p}\cdot\vec{x}}-1)e^{-i\vec{p}\cdot\vec{x}'}. \tag{A14}$$

The required thermal average is thus

$$\langle e^{i\vec{Q}\cdot[\vec{u}(\vec{x})-\vec{u}(\vec{0})]}\rangle_0 = \exp\left[-\tfrac{1}{2}Q_iQ_jU_{ij}(\vec{x})-\frac{i\gamma}{k_BT}Q_j\int d^3x'\,\delta c(\vec{x}')V_j(\vec{x}',\vec{x})\right]. \tag{A15}$$

To carry out the remaining quenched average in Eq. (A11) we need to evaluate

$$\overline{\exp\left[\frac{-i\gamma}{k_BT}Q_j\int d^3x'\,\delta c(\vec{x}')V_j(\vec{x}',x)\right]}, \tag{A16}$$

which, using Eq. (A7), is readily found to be equal to

$$\exp\left[-\frac{1}{2}\frac{\gamma^2}{(2\mu+\lambda)}Q_iQ_jW_{ij}(\vec{x})\right], \tag{A17}$$

where

$$W_{ij}(\vec{x})=\frac{2k_BT_q}{\Delta}\frac{1}{V}\sum_{\vec{p}}\frac{p_ip_j}{p^4}(1-e^{i\vec{p}\cdot\vec{x}}). \tag{A18}$$

Combining everything together, we have finally

$$\overline{\langle e^{i\vec{Q}\cdot[\vec{u}(\vec{x})-\vec{u}(\vec{0})]}\rangle} = \exp\left\{-Q_iQ_j\frac{1}{V}\sum_{\vec{p}}\frac{1}{p^2}(1-e^{i\vec{p}\cdot\vec{x}})\left[\frac{k_BT}{\mu}\left[\delta_{ij}-\frac{p_ip_j}{p^2}\right]+\left[\frac{k_BT}{2\mu+\lambda}+\frac{k_BT_q\gamma^2}{\Delta(2\mu+\lambda)^2}\right]\frac{p_ip_j}{p^2}\right]\right\}. \tag{A19}$$

The small $\vec{k}$ behavior of the structure factor (A11) is dominated by the large $\vec{x}$ behavior of the averages discussed above. The term of (A19) proportional to $e^{i\vec{p}\cdot\vec{x}}$, in particular, behaves like $1/x$ for large x, and can be expanded down from the exponential. Upon inserting Eq. (A19) into Eq. (A11) and expanding in this way, we obtain our final result:

$$S(\vec{q})\propto e^{-Q^2\overline{\langle|\vec{u}(\vec{x})|^2\rangle}}\left\{\delta(\vec{k})+\frac{Q_iQ_j}{k^2}\left[\frac{k_BT}{\mu}\left[\delta_{ij}-\frac{k_ik_j}{k^2}\right]+\left[\frac{k_BT}{2\mu+\lambda}+\frac{k_BT_q\gamma^2}{\Delta(2\mu+\lambda)^2}\right]\frac{k_ik_j}{k^2}\right]\right\}, \tag{A20}$$

where the Debye-Waller prefactor

$$\overline{\langle|\vec{u}(\vec{x})|^2\rangle}=\left[\frac{5\mu+2\lambda}{3\mu(2\mu+\lambda)}k_BT+\frac{\gamma^2k_BT_q}{3\Delta(2\mu+\lambda)^2}\right]\times\frac{1}{V}\sum_{\vec{p}}\left[\frac{1}{p^2}\right]. \tag{A21}$$

Passing to limit of large volumes V and setting $T=0$ we obtain the result (1.9) quoted in the Introduction.

APPENDIX B: STRUCTURE FACTOR FORMULA

In this Appendix we shall derive formulas (2.30)–(2.33) and also Eq. (2.41) for the case of quenched phasons. As a preliminary step, we must prove two simple formulas,

$$\sum_{\mathbf{Q}}\delta(\mathbf{q}-\mathbf{Q})=\frac{v_c}{(2\pi)^d}\sum_{\mathbf{R}}e^{i\mathbf{q}\cdot\mathbf{R}}, \tag{B1}$$

where $\mathbf{R}$ is a vector of a hyperlattice whose unit-cell volume is v_c while $\mathbf{Q}$ is a vector of the corresponding reciprocal hyperlattice, and

$$\delta^{\parallel}(\mathbf{q}^{\parallel}=\mathbf{0})=N^{\parallel}\frac{v_c}{v^{\perp}(2\pi)^3}, \tag{B2}$$

where $v^{\perp}$ is volume of a domain in $\perp$ subspace which decorates every hyperlattice point, and $N^{\parallel}$ is the number of intersections of these domains with the physical, $\parallel$ subspace. The first formula can be proved by integrating both sides of this equation over a reciprocal unit cell. The second formula can be proved by setting $\mathbf{q}^{\parallel}=\mathbf{0}$ in Eq.

(B1) and then integrating both sides over $\mathbf{q}^\perp$ with the weight

$$w(\mathbf{q}^\perp)\equiv\int_{v^\perp}\exp(-i\mathbf{q}^\perp\cdot\mathbf{x}^\perp)d^{d-3}x^\perp\ . \tag{B3}$$

This weight is the $\perp$ Fourier transform of the function

$$W(\mathbf{x}^\perp)=\begin{cases}1, & \mathbf{x}^\perp\in v^\perp\\ 0 & \text{otherwise}\ .\end{cases} \tag{B4}$$

In deriving Eq. (B2) it is necessary to recall that $\mathbf{Q}=\mathbf{0}\Longleftrightarrow\mathbf{Q}^\parallel=\mathbf{0}\Longleftrightarrow\mathbf{Q}^\perp=\mathbf{0}$, and to observe that

$$N^\parallel=\sum_{\mathbf{R}}W(\mathbf{R}^\perp)\ . \tag{B5}$$

There are two immediate consequences of Eq. (B2). First, the usual substitution for the square of the delta function,

$$[\delta(\mathbf{q})]^2=N\frac{v_c}{(2\pi)^3}\delta(\mathbf{q})\ , \tag{B6}$$

used for periodic lattices, generalizes to

$$[\delta^\parallel(\mathbf{q}^\parallel)]^2=N^\parallel\frac{v_c}{v^\perp(2\pi)^3}\delta^\parallel(\mathbf{q}^\parallel)\ , \tag{B7}$$

in the case of quasilattices. Second, since $v^\perp$ is arbitrary, Eq. (B2) implies that points $\{\mathbf{R}^\perp\}$ fill $\perp$ space uniformly.

Using the standard results for Gaussian integrations the average in Eq. (2.27) can be easily evaluated,

$$f=\exp\left[-\tfrac{1}{4}\int(\mathbf{k}_2e^{-i\mathbf{p}^\parallel\cdot\mathbf{R}_2^\parallel}-\mathbf{k}_1e^{-i\mathbf{p}^\parallel\cdot\mathbf{R}_1^\parallel})\cdot\mathbf{C}^{-1}(\mathbf{p}^\parallel)\cdot(\mathbf{k}_2e^{i\mathbf{p}^\parallel\cdot\mathbf{R}_2^\parallel}-\mathbf{k}_1e^{i\mathbf{p}^\parallel\cdot\mathbf{R}_1^\parallel})d^3p^\parallel\right]\ , \tag{B8}$$

and can be seen to depend only on the difference $\mathbf{R}_1-\mathbf{R}_2$. This can be used to simplify the structure factor in Eq. (2.26). We first make the substitution

$$\mathbf{R}_1-\mathbf{R}_2\rightarrow\mathbf{R}\ ,$$
$$\mathbf{R}_2\rightarrow\mathbf{R}'\ . \tag{B9}$$

Then, by using (B1), summation over $\mathbf{R}'$ can be immediately carried out to give the factor

$$\frac{(2\pi)^d}{v_c}\sum_{\mathbf{Q}}\delta(\mathbf{k}_1-\mathbf{k}_2-\mathbf{Q})\ . \tag{B10}$$

However, since the two $\delta^\parallel$'s in Eq. (2.26) force $\mathbf{k}_1^\parallel=\mathbf{k}_2^\parallel=\mathbf{q}^\parallel$, and since $\mathbf{Q}^\parallel=\mathbf{0}\Longleftrightarrow\mathbf{Q}=\mathbf{0}$, the only term surviving in the above sum is the $\mathbf{Q}=\mathbf{0}$ term. Therefore, the integral over one of the $\mathbf{k}$'s can be performed, and after applying Eq. (B7) we are left with

$$S^\parallel(\mathbf{q}^\parallel)=v^\perp(2\pi)^{d-3}\sum_{\mathbf{R}}\int e^{-i\mathbf{k}\cdot\mathbf{R}}f(\mathbf{R},\mathbf{k})\mid W(\mathbf{k})\mid^2\times\delta^\parallel(\mathbf{q}^\parallel-\mathbf{k}^\parallel)d^dk\ , \tag{B11}$$

where

$$f(\mathbf{R},\mathbf{k})=\exp\left[-\tfrac{1}{2}\mathbf{k}\cdot\left[\int[1-\cos(\mathbf{p}^\parallel\cdot\mathbf{R}^\parallel)]\times\mathbf{C}^{-1}(\mathbf{p}^\parallel)d^3p^\parallel\right]\cdot\mathbf{k}\right] \tag{B12}$$

follows from Eq. (B8) with substitutions $\mathbf{k}_1=\mathbf{k}_2=\mathbf{k}$ and $\mathbf{R}_1-\mathbf{R}_2=\mathbf{R}$.

In order to evaluate the remaining sum and integral in Eq. (B11), we first observe that the integral in Eq. (B12) is dominated by the contribution from the first term in the integrand since the positive and the negative contributions from the cosine will tend to cancel each other. Therefore we can expand the exponent to obtain

$$f(\mathbf{R},\mathbf{k})=f_0(\mathbf{k})[1+f_1(\mathbf{R},\mathbf{k})+\cdots]\ , \tag{B13}$$

where

$$f_0(\mathbf{k})=\exp\left[-\tfrac{1}{2}\mathbf{k}\cdot\left[\int\mathbf{C}^{-1}(\mathbf{p}^\parallel)d^3p^\parallel\right]\cdot\mathbf{k}\right]\ , \tag{B14}$$

and

$$f_1(\mathbf{R},\mathbf{k})=\tfrac{1}{2}\mathbf{k}\cdot\left[\int\cos(\mathbf{p}^\parallel\cdot\mathbf{R}^\parallel)\mathbf{C}^{-1}(\mathbf{p}^\parallel)d^3p^\parallel\right]\cdot\mathbf{k}\ . \tag{B15}$$

Associated expansion of the structure factor Eq. (B11) is

$$S^\parallel(\mathbf{q}^\parallel)=S_0^\parallel(\mathbf{q}^\parallel)+S_1^\parallel(\mathbf{q}^\parallel)+\cdots\ , \tag{B16}$$

where

$$S_0^\parallel(\mathbf{q}^\parallel)=v^\perp(2\pi)^{d-3}\sum_{\mathbf{R}}\int e^{-i\mathbf{k}\cdot\mathbf{R}}f_0(\mathbf{k})\mid W(\mathbf{k})\mid^2\times\delta^\parallel(\mathbf{q}^\parallel-\mathbf{k}^\parallel)d^dk\ , \tag{B17}$$

and

$$S_1^\parallel(\mathbf{q}^\parallel)=v^\perp(2\pi)^{d-3}\sum_{\mathbf{R}}\int e^{-i\mathbf{k}\cdot\mathbf{R}}f_0(\mathbf{k})f_1(\mathbf{R},\mathbf{k})\mid W(\mathbf{k})\mid^2\times\delta^\parallel(\mathbf{q}^\parallel-\mathbf{k}^\parallel)d^dk\ . \tag{B18}$$

The zeroth-order contribution to the structure factor, Eq. (B17), can be easily evaluated by using Eq. (B1). This gives Eq. (2.31) and we see that $f_0(\mathbf{Q})$ is analogous to the usual Debye-Waller factor. $f_0(\mathbf{Q})$ is Gaussian in the physical $\mathbf{Q}^\parallel$ as well as in the complementary $\mathbf{Q}^\perp$ components of the diffraction vector. Of course, since there is a one-to-one correspondence between $\mathbf{Q}^\parallel$ and $\mathbf{Q}^\perp$, one could view f_0 as a function only of $\mathbf{Q}^\parallel$. However, an important difference from the usual Debye-Waller factor is that for a quasicrystal this would be a highly irregular function of $\mathbf{Q}^\parallel$.

In analogy to ordinary crystals, we expect that $S_1(\mathbf{q}^\parallel)$ describes diffuse, Huang scattering characterized by algebraic peaks overlapping the usual Bragg, δ-function peaks. Indeed, this is the case, as can be seen by explicitly evaluating Eq. (B18). The sum in this equation can be evaluated by writing the cosine as the sum of two exponentials and, then, using once more Eq. (B1). The resulting δ function and already present $\delta^\parallel$ function make the integrals over $\mathbf{k}$ and $\mathbf{p}^\parallel$ trivial so that we obtain Eq. (2.32).

We shall conclude this section by sketching derivation of the effective hydrodynamic matric $\mathbf{C}_{\rm eff}(\mathbf{p}^{\parallel})$ appropriate for the case of quenched phasons. The average of

$$\exp[i\mathbf{k}_2\cdot\mathbf{u}(\mathbf{R}_2)-i\mathbf{k}_1\cdot\mathbf{u}(\mathbf{R}_1)]$$

now involves first averaging over $P_{\rm eff}[\mathbf{u}^{\parallel}]$ given in Eq. (2.38) and then over $P_q[\mathbf{u}_q^{\perp}]$ given in Eq. (2.40). The two averaging steps are not independent because of the $\mathbf{u}_q^{\perp}$ dependence in the normalization of $P_{\rm eff}$. However, the two steps can be made independent if a change of variables is made in the first integration,

$$\mathbf{u}^{\parallel}\rightarrow\bar{\mathbf{u}}^{\parallel}=\mathbf{u}^{\parallel}+[\mathbf{C}^{\parallel,\parallel}]^{-1}\cdot\mathbf{C}^{\parallel,\perp}\cdot\mathbf{u}_q^{\perp}\ . \tag{B19}$$

Now, by completing the usual Gaussian averages one finds the same results as in (B8), except that $\mathbf{C}^{-1}$ is replaced by

$$\mathbf{C}_{\rm eff}^{-1}=\begin{bmatrix}(\mathbf{C}^{\parallel,\parallel})^{-1}+(\mathbf{C}^{\parallel,\parallel})^{-1}\cdot\mathbf{C}^{\parallel,\perp}\cdot(\mathbf{C}_q^{\perp\perp})^{-1}\cdot\mathbf{C}^{\perp,\parallel}\cdot(\mathbf{C}^{\parallel,\parallel})^{-1} & -(\mathbf{C}^{\parallel,\parallel})^{-1}\cdot\mathbf{C}^{\parallel,\perp}\cdot(\mathbf{C}_q^{\perp,\perp})^{-1}\\ -(\mathbf{C}_q^{\perp,\perp})^{-1}\cdot\mathbf{C}^{\perp,\parallel}\cdot(\mathbf{C}^{\parallel,\parallel})^{-1} & (\mathbf{C}_q^{\perp,\perp})^{-1}\end{bmatrix}, \tag{B20}$$

where we suppressed the implicit $p^{\parallel}$ dependence. By inverting the last equation it can be verified that

$$\mathbf{C}_{\rm eff}=\begin{bmatrix}\mathbf{C}^{\parallel,\parallel} & \mathbf{C}^{\parallel,\perp}\\ \mathbf{C}^{\perp,\parallel} & \mathbf{C}_q^{\perp,\perp}+\mathbf{C}^{\perp,\parallel}\cdot(\mathbf{C}^{\parallel,\parallel})^{-1}\cdot\mathbf{C}^{\parallel,\perp}\end{bmatrix},$$

as claimed in Eq. (2.41).

APPENDIX C: COORDINATE SYSTEMS FOR ICOSAHEDRAL GROUP

The orientation of the icosahedral group with respect to the coordinate axes in the physical and the complementary spaces can be specified by the projections (components) of the six orthonormal vectors $\hat{\mathbf{e}}_\mu$, $\mu=1,2,\ldots,6$, which generate the six-dimensional hypercubic lattice.[27] In the $\parallel$, physical space, we specify these projections in the following way:

$$\begin{aligned}
&\mathbf{e}_1^{\parallel}=\eta(\tau,0,1)\ ,\\
&\mathbf{e}_2^{\parallel}=\eta(\tau,0,-1)\ ,\\
&\mathbf{e}_3^{\parallel}=\eta(1,\tau,0)\ ,\\
&\mathbf{e}_4^{\parallel}=\eta(0,1,\tau)\ ,\\
&\mathbf{e}_5^{\parallel}=\eta(0,-1,\tau)\ ,\\
&\mathbf{e}_6^{\parallel}=\eta(1,-\tau,0)\ .
\end{aligned} \tag{C1}$$

Similarly, in the $\perp$, complementary space we specify

$$\begin{aligned}
&\mathbf{e}_1^{\perp}=\eta(1,0,-\tau)\ ,\\
&\mathbf{e}_2^{\perp}=\eta(1,0,\tau)\ ,\\
&\mathbf{e}_3^{\perp}=\eta(-\tau,1,0)\ ,\\
&\mathbf{e}_4^{\perp}=\eta(0,-\tau,1)\ ,\\
&\mathbf{e}_5^{\perp}=\eta(0,\tau,1)\ ,\\
&\mathbf{e}_6^{\perp}=\eta(-\tau,-1,0)\ .
\end{aligned} \tag{C2}$$

The projections of the unit vectors will have magnitude $1/\sqrt{2}$, so that

$$\eta=1/\sqrt{2\tau+4}\ , \tag{C3}$$

where $\tau=\frac{1}{2}(1+\sqrt{5})$ is the golden mean.

Our choice of the orientations of the icosahedral group is guided by the fact that icosahedral group has tetrahedral group as its subgroup. We choose the orientations so that the two inequivalent representations of the icosahedral group, spanned by $\parallel$ and $\perp$ subspaces are *identical* when restricted to a tetrahedral subgroup. Orientation of the tetrahedral subgroup is a standard one, with the coordinate axes coinciding with the twofold axes. This facilitates efficient extension of the available results from tetrahedral to icosahedral symmetry. Obviously, selection of a particular permutation of the basis is irrelevant to the above point.

With the above orientation, a hyperlattice vector

$$\mathbf{R}=an_\mu\hat{\mathbf{e}}_\mu\ , \tag{C4}$$

where a is the hyperlattice constant and n_μ are integers, has projections

$$\mathbf{R}^{\parallel}=an_\mu\mathbf{e}_\mu^{\parallel} \tag{C5}$$

and

$$\mathbf{R}^{\perp}=an_\mu\mathbf{e}_\mu^{\perp}\ . \tag{C6}$$

Similarly, a reciprocal hyperlattice vector

$$\mathbf{Q}=\frac{2\pi}{a}l_\mu\hat{\mathbf{e}}_\mu \tag{C7}$$

has projections

$$\mathbf{Q}^{\parallel}=\frac{2\pi}{a}l_\mu\mathbf{e}_\mu^{\parallel} \tag{C8}$$

and

$$\mathbf{Q}^{\perp}=\frac{2\pi}{a}l_\mu\mathbf{e}_\mu^{\perp}\ . \tag{C9}$$

Integers l_μ can be used to index Bragg peaks of icosahedral quasicrystals.

In order to obtain an icosahedral quasicrystal with atoms at the vertices of the Ammann quasilattice, one decorates hyperlattice vertices with "flat" surfaces

$$\mathbf{s}^{\parallel}(\boldsymbol{\xi}^{\perp})\equiv\mathbf{0}\ , \tag{C10}$$

whose shape in $\perp$ space is a rhombic triacontahedron with edges $\pm a\mathbf{e}_\mu^{\perp}$, that is, the projection of the unit hypercube.

Consequently,

$$v^{\perp}=(10+4\sqrt{5})^{1/2}a^3\approx 4.352\,50a^3\ . \tag{C11}$$

In order to establish a correspondence with coordinate systems of other authors, it is generally necessary to first make a correspondence between the labelings of the six vectors e_μ, and then give transformations between the coordinate frames. For example, if we denote vectors and coordinates given in Ref. 25 by an overbar, the following transformation can be established:

$$\begin{bmatrix} e_1 \\ e_2 \\ e_3 \\ e_4 \\ e_5 \\ e_6 \end{bmatrix} = \begin{bmatrix} -1 & 0 & 0 & 0 & 0 & 0 \\ 0 & 1 & 0 & 0 & 0 & 0 \\ 0 & 0 & 0 & 1 & 0 & 0 \\ 0 & 0 & 0 & 0 & 0 & 1 \\ 0 & 0 & 1 & 0 & 0 & 0 \\ 0 & 0 & 0 & 0 & 1 & 0 \end{bmatrix} \begin{bmatrix} \bar{e}_1 \\ \bar{e}_2 \\ \bar{e}_3 \\ \bar{e}_4 \\ \bar{e}_5 \\ \bar{e}_6 \end{bmatrix}, \tag{C12}$$

$$\begin{bmatrix} x_1^{\parallel} \\ x_2^{\parallel} \\ x_3^{\parallel} \end{bmatrix} = \begin{bmatrix} 0 & 0 & 1 \\ 0 & 1 & 0 \\ -1 & 0 & 0 \end{bmatrix} \begin{bmatrix} \bar{x}_1^{\parallel} \\ \bar{x}_2^{\parallel} \\ \bar{x}_3^{\parallel} \end{bmatrix}, \tag{C13}$$

and

$$\begin{bmatrix} x_1^{\perp} \\ x_2^{\perp} \\ x_3^{\perp} \end{bmatrix} = \begin{bmatrix} -1 & 0 & 0 \\ 0 & 1 & 0 \\ 0 & 0 & -1 \end{bmatrix} \begin{bmatrix} \bar{x}_1^{\perp} \\ \bar{x}_2^{\perp} \\ \bar{x}_3^{\perp} \end{bmatrix}. \tag{C14}$$

Obviously, the first transformation is not unique, but once chosen it uniquely fixed the coordinate transformations. If the first transformation is changed by an element of the icosahedral group, the coordinate transformations must be changed by the same element.

[1]D. R. Nelson and B. I. Halperin, Science **229**, 233 (1985).

[2]C. Henley, Comments Condens. Matter Phys. **13**, 59 (1987).

[3]Proceedings of the International Workshop on Aperiodic Crystals, edited by D. Gratias and L. Michel [J. Phys. (Paris) Colloq. **47**, No. 3 (1986)].

[4]P. J. Steinhardt and S. Ostlund, *The Physics of Quasicrystals* (World-Scientific, Singapore, 1988).

[5]*Introduction to Quasicrystals* and *Introduction to Mathematics of Quasicrystals*, Vols. 1 and 2 of *Aperiodicity and Order*, edited by M. V. Jarić (Academic, Boston, 1988).

[6]D. Shechtman, I. Blech, D. Gratias, and J. W. Cahn, Phys. Rev. Lett. **53**, 1951 (1984).

[7]D. Levine and P. J. Steinhardt, Phys. Rev. Lett. **53**, 2477 (1984).

[8]R. Ammann (unpublished); see also A. L. Mackay, Kristallografiya **26**, 910 (1981) [Sov. Phys.—Crystallogr. **26**, 517 (1981)]; P. Kramer and R. Neri, Acta Crystallogr. Sect. A **40**, 580 (1984).

[9]R. Penrose, Bull. Inst. Math. Appl. **10**, 216 (1974); see also M. Gardner, Sci. Am. **236**(1), 110 (1977); B. Grünbaum and T. Shephard, *Tilings of the Plane* (Freeman, San Francisco, 1987).

[10]V. Elser and C. L. Henley, Phys. Rev. Lett. **55**, 2883 (1985); P. Guyot and M. Audier, Philos. Mag. B **52**, L15 (1985); M. Audier and P. Guyot, *ibid.* **53**, 143 (1986).

[11]C. L. Henley and V. Elser, Philos. Mag. B **53**, 159 (1986).

[12]P. A. Kalugin, A. Yu. Kitaev. and L. S. Levitov, Pis'ma Zh. Eksp. Teor. Fiz. **41**, 119 (1985) [JETP Lett. **41**, 145 (1985)]; M. Duneau and A. Katz, Phys. Rev. Lett. **54**, 2688 (1985); V. Elser, Phys. Rev. B **32**, 4892 (1985); Acta Crystallogr. Sect. A **42**, 36 (1986).

[13]V. Elser, Phys. Rev. Lett. **54**, 1730 (1985).

[14]P. A. Bancel and P. Heiney, J. Phys. (Paris) Colloq. **47**, C3-341 (1986); T. C. Lubensky, J. E. S. Socolar, P. J. Steinhardt, P. A. Bancel, and P. A. Heiney, Phys. Rev. Lett. **57**, 1440 (1986); P. M. Horn, W. Malzfeldt, D. P. DiVincenzo, J. Toner, and R. Gambino, *ibid.* **57**, 1444 (1986).

[15]P. A. Bancel, P. A. Heiney, P. W. Stephens, A. E. Goldman, and P. M. Horn, Phys. Rev. Lett. **54**, 2422 (1985).

[16]P. A. Heiney, P. A. Bancel, P. M. Horn, J. L. Jordan, S. LaPlaca, J. Angilello, and F. W. Gayle, Science **238**, 660 (1987).

[17]D. Shechtman, and I. A. Blech, Metall. Trans. **16A**, 1005 (1985); P. W. Stephens and A. I. Goldman, Phys. Rev. Lett. **56**, 1168 (1986).

[18]V. Elser, in *Proceedings of the XVth International Colloquium on Group Theoretical Methods in Physics*, edited by R. Gilmore (World-Scientific, Singapore, 1987), Vol. 1, p. 162.

[19]For a preliminary report on some of our results, see M. V. Jarić, J. Phys. (Paris) Colloq. **47**, C3-259 (1986).

[20]J. E. S. Socolar and D. C. Wright, Phys. Rev. Lett. **59**, 221 (1987).

[21]M. A. Krivoglaz, *Theory of X-Ray and Thermal-Neutron Scattering by Real Crystals* (Plenum, New York, 1969). This reference contains an excellent account of how dislocations, substitutional disorder, and other realistic perturbations affect the scattering in otherwise perfect crystals.

[22]S. Moss and P. Horn (private communication).

[23]T. C. Lubensky, S. Ramaswamy, and J. Toner, Phys. Rev. B **32**, 7444 (1985).

[24]P. Bak, Phys. Rev. Lett. **54**, 1517 (1985); Phys. Rev. B **32**, 5764 (1985).

[25]D. Levine, T. C. Lubensky, S. Ostlund, S. Ramaswamy, P. J. Steinhardt, and J. Toner, Phys. Rev. Lett. **54**, 1520 (1985).

[26]P. A. Kalugin, A. Yu. Kitayev, and L. S. Levitov, J. Phys. (Paris) Lett. **46**, L601 (1985).

[27]M. V. Jarić, in *Proceedings of the XVth International Colloquium on Group Theoretical Methods in Physics*, edited by R. Gilmore (World-Scientific, Singapore, 1987).

[28]Our choice of orientation of the icosahedral symmetry axes in physical (phonon) space and in the perpendicular (phason) space is described in Sec. III [see also M. V. Jarić, J. Phys. (Paris) Colloq. **47**, C3-82 (1987) and Ref. 27]. A connection with orientations of Refs. 23–26 is described in Appendix C.

[29]D. R. Nelson, Phys. Rev. B **27**, 2902 (1983); this reference discusses the interplay between Huang scattering and theories of dislocation mediated melting in two dimensions.

[30]J. W. Cahn, D. Shechtman, and D. Gratias, J. Mater. Res. **1**, 13 (1986).

[31]We use here an arrow to denote three-dimensional vectors. Note, however, that although $\vec{Q}^{\perp}$ is a three-dimensional vector, it is not from the physical space but rather from its complement, the $\perp$ subspace. More general notation will be used in Secs. II and III, where formulas (1.12) and (1.15) will be derived.

[32]M. V. Jarić and U. Mohanty, Phys. Rev. Lett. **58**, 230 (1987); Phys. Rev. B **37**, 4441 (1988).

[33]S. Sachdev and D. R. Nelson, Phys. Rev. B **32**, 4592 (1985).

[34]Certain combinations of elastic constants arising in a density-functional calculation of quasicrystal stability (Ref. 33) have been used previously in a different context to estimate the dependence of peak widths on $\mathbf{Q}^{\perp}$ (see Refs. 11 and 16).

[35]In this paper we derive formulas for simple quasicrystals. For decorated quasilattices, the derived formulas need to be generalized in a similar way as for the Bragg scattering from quasicrystals [M. V. Jarić, Phys. Rev. B **34**, 4685 (1986)].

[36]P. M. DeWolff, Acta Crystallogr. Sect. A **30**, 777 (1974).

[37]A. Janner and T. Janssen, Phys. Rev. B **15**, 643 (1977); Physica (Amsterdam) **99A**, 47 (1979).

[38]N. G. deBruijn, Ned. Akad. Weten. Proc. Ser. A **43**, 39, 53 (1981).

[39]P. Bak, Phys. Rev. Lett. **56**, 861 (1986).

[40]D. M. Frenkel, C. Henley, and E. Siggia, Phys. Rev. B **34**, 3649 (1986).

[41]Just as the unit cell of a periodic crystal cannot be uniquely defined, the definition of $v^{\perp}$ is not unique. The domain $v^{\perp}$ can be arbitrarily restricted, providing the function $\mathbf{s}^{\parallel}$ is made multivalued. In such a case, as when there is more than one atomic species, a sum over different sheets of $\mathbf{s}^{\parallel}$ must be introduced. We shall assume throughout that $\mathbf{s}^{\parallel}$ is singlevalued.

[42]Although F is continuous as $\partial \mathbf{u}^{\perp}/\partial \mathbf{x}^{\parallel} \rightarrow 0$, this does not imply that phasons are appropriate hydrodynamic variables. Whether phasons are pinned or not is a question of dynamics and depends on the energy barriers (landscape) in the configuration space.

[43]Our particular form of the five basic matrices $\hat{\mathbf{C}}_i$ (which are not orthonormalized) is dictated by our choice in Ref. 27 of the five basic, orthonormalized elastic modulus tensors $\hat{\mathbf{M}}_i$. Using coordinate relationships given in Appendix C, it can be verified that these matrices agree with ones given in Refs. 23–26.

[44]T. Ichikawa, Phys. Status Solidi A **19**, 707 (1973).

[45]For example, for Fe, Co, and Ni, T_m is around 1800 K, while estimated T_g is around 600 K.